New Organic Dye Based on a 3,6-Disubstituted Carbazole Donor for Efficient Dye-Sensitized Solar Cells

Woochul Lee,[a] Nara Cho,[b] Jongchul Kwon,[a] Jaejung Ko,*[b] and Jong-In Hong*[a]

Dedicated to Professor Eun Lee on the occasion of his retirement and 65th birthday

Abstract: We have synthesized and characterized four organic dyes (**H1–H4**) based on a 3,6-disubstituted carbazole donor as sensitizers in dye-sensitized solar cells. These dyes have high molar extinction coefficients and energy levels suitable for electron transfer from an electrolyte to nanocrystalline TiO_2 particles. Under standard air mass 1.5 global (AM 1.5G) solar irradiation, a device using dye **H4** exhibits a short-circuit current density (J_{sc}) of 13.7 mA cm^{-2}, an open-circuit voltage (V_{oc}) of 0.68 V, a fill factor (*FF*) of 0.70, and a calculated efficiency of 6.52%. This performance is comparable to that of a reference cell based on N719 (7.30%) under the same conditions. After 1000 hours of visible-light soaking at 60°C, the overall efficiency remained at 95% of the initial value.

Keywords: electrochemistry · electron transfer · sensitizers · solar cells · substituted carbazole

Introduction

Solar energy has infinite potential to address the challenges of global warming and declining fossil fuel resources because it is renewable and offers unlimited access.[1] In recent years, considerable effort has been devoted to converting photo energy into electrically available energy using solar cells. Among several types of photovoltaic devices, dye-sensitized solar cells (DSCs) have attracted a great deal of attention owing to their low production cost and relatively high energy conversion efficiency.[2] Conventional DSCs typically consist of nanocrystalline titanium oxide, a sensitizer, and an electrolyte.[3] Of these, the photosensitizer is crucial for realizing highly efficient DSCs. Ruthenium-based sensitizers, such as N3,[1,4,5] N719,[6] and black dye,[7] have achieved efficiencies of up to 11% under air mass 1.5 global (AM 1.5G) irradiation. However, ruthenium-based sensitizers have some drawbacks, such as low molecular extinction coefficients and costly synthesis and purification.[8] Metal-free organic dyes are an attractive alternative because they offer high absorption, diverse structures, low material cost, and ease of purification.[5,9,10]

Certain fundamental requirements must be met when designing highly efficient sensitizers. First, efficient sensitizers should have good light-harvesting ability, which is related to the molecular extinction coefficient and the overlap of the dye absorption with the solar spectrum. To improve their light-harvesting ability, dyes should have a high absorptivity and a greater absorption in the visible region. Second, to achieve efficient electron injection from the excited dye to the conduction band of TiO_2, the lowest unoccupied molecular orbital (LUMO) of the sensitizer must be more negative than the conduction band of the nanoporous metal oxide. On the other hand, the highest occupied molecular orbital (HOMO) of the sensitizer must be more positive than the redox potential of the electrolyte chosen, such as I^-/I_3^-, for rapid electron injection into the oxidized dye.

Many organic dyes have recently been designed and synthesized, including coumarin,[11] indoline,[9,12] porphyrin,[13] merocyanine,[14] squaraine,[15] and oligothiophene, which usually contain triphenylamine (TPA) or difluorenylamine as an electron donor.[16] Among these various molecular structures, a maximum efficiency of about 9.5% was achieved with an indoline dye.[12a] Further, a strikingly high efficiency of 10% was reported when electron-rich 3,4-ethylenedioxythiophene was combined with dihexyl-substituted dithienosilole as a linker between the donor and the anchoring unit.[17] TPA moieties, which have good electron-donating ability as well as hole-transporting properties, have been frequently used as the donor unit.[18]

In this study, we synthesized and characterized four organic dyes consisting of 3,6-bis(triphenylamine)-substituted carbazole, dithiophene, and cyanocarboxylic acid as an anchoring group to bind to TiO_2 nanoparticles. The photophysical and electrochemical properties and device performance of the sensitizers were systematically investigated. The ab-

[a] W. Lee, J. Kwon, Prof. Dr. J.-I. Hong
Department of Chemistry
Seoul National University
Seoul 151-747 (Korea)
Fax: (+82) 02-889-1568
E-mail: jihong@snu.ac.kr

[b] N. Cho, Prof. Dr. J. Ko
Department of New Material Chemistry
Korea University
Jochiwon, Chungnam 339-700 (Korea)

Supporting information for this article is available on the WWW under http://dx.doi.org/10.1002/asia.201100661.

sorption peaks were red-shifted and better matched to the solar spectrum by extending the conjugation length between the donor and bridge units, which contributed to an increase in the short-circuit current (J_{sc}) . The molar extinction coefficients of the four dyes varied with the conjugation length. Energy levels suitable for efficient electron transfer from an electrolyte to nanocrystalline TiO_2 particles were also obtained by controlling the conjugation length and donor group. The best performance obtained in this study was 6.52% for the dye with the longest conjugation length between the donor and the bridge group, **H4**. This dye also showed good long-term stability.

Results and Discussion

The molecular structures of the dyes and their syntheses are shown in Schemes 1 and 2, respectively. Compounds **1**, **3**, **8**, and **10** were synthesized by a palladium-catalyzed Suzuki re-
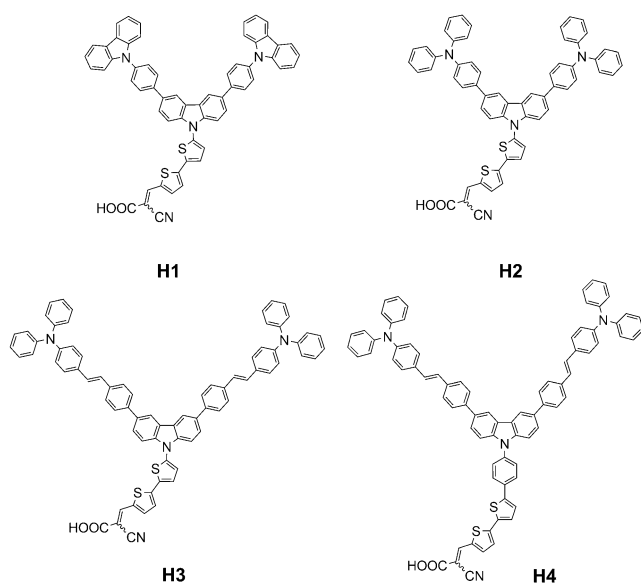
Scheme 1. Molecular structures of the organic dyes.

action, and compound **5** was synthesized by the Heck C–C coupling reaction of **10**. Compounds **2**, **4**, **6**, and **7** were prepared from compound **8** by the copper-catalyzed Ullmann coupling reaction, and compound **9** was prepared by the Vilsmeier–Haack formylation of compound **8**. Finally, all the sensitizers were obtained as a mixture of *E/Z* isomers by the Knoevenagel condensation reaction between cyanoacetic acid and formylated intermediates. A representative experimental protocol is described in the Experimental Section.

The UV/Vis absorption spectra of sensitizers **H1–H4** are shown in Figure 1, and their photophysical data are listed in Table 1. As shown in Figure 1, **H2** exhibits an improved red shift of its absorption spectrum in the range of 375–475 nm
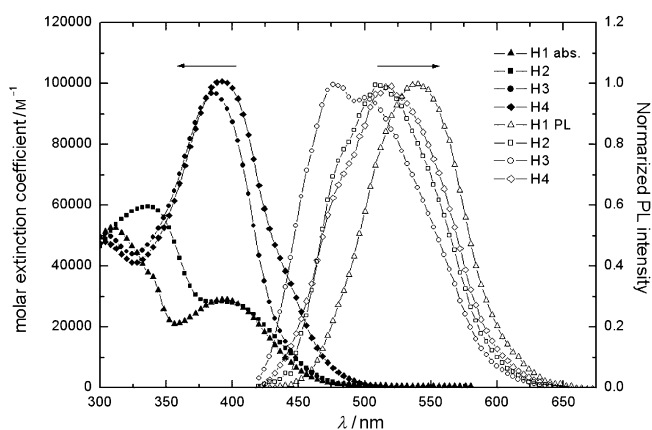

Figure 1. Absorption and photoluminescence spectra of sensitizers **H1–H4** in a DMF solution.

when compared with **H1**, owing to the better electron-donating ability of TPA. The difference in the molar extinction coefficients of **H1** and **H2** at 300–375 nm can be attributed to the π–π* transition of the conjugated system, which depends on the absorbance of the electron donor unit. Under the same conditions, a TPA moiety is more suitable as a donor group in terms of its light harvesting ability. The absorption bands of **H3** and **H4** are more intense and broader than those of **H1** and **H2**. Extending the conjugated system by the addition of a phenylvinylene unit at the carbazole core leads to a shift in absorption onset to longer wavelength. In addition, sensitizer **H4**, which has phenyldithiophene as a bridging group, shows the highest molecular extinction coefficient at its maximum absorption values ($\lambda_{max} = 390$ nm, $\epsilon > 100\,000\,M^{-1}\,cm^{-1}$) and the longest wavelength absorption band reaching up to 500 nm. In addition, the **H4** dye also shows stronger and broadened UV/Vis absorption bands when adsorbed on a TiO_2 film (Figure S1 in the Supporting Information). These results imply that the electron-donating substituents at the 3- and 6-positions of the carbazole ring contribute to its light-harvesting ability. Thus, **H4** exhibits the best molar absorptivity and absorption range for visible light. The electrochemical properties of these sensitizers were determined by using cyclic voltammetry in a *N,N*-dimethylformamide (DMF) solution containing tetrabutylammonium hexafluorophosphate ($TBAPF_6$) as a supporting electrolyte (Table 1). Dyes **H2–H4** show similar electrochemical profiles with quasi-reversible waves; their recorded oxidation potentials are 1.11, 0.97, and 1.01 V, respectively, versus the normal hydrogen electrode (NHE) (Figure S2 in the Supporting Information). However, **H1** exhibits an irreversible oxidation potential. Slight changes in the oxidation potentials of about 0.1 V appear between **H2** and **H3** (or **H4**) owing to the increase in π-conjugation length in the dyes. For **H1**, it is more difficult to regenerate the oxidized sensitizer (compared to the redox potential of the electrolyte) when compared to the other H dyes because of the incorporation of a phenylcarbazole moiety into the 3- and 6-positions of the carbazole core, which lowers the oxidation
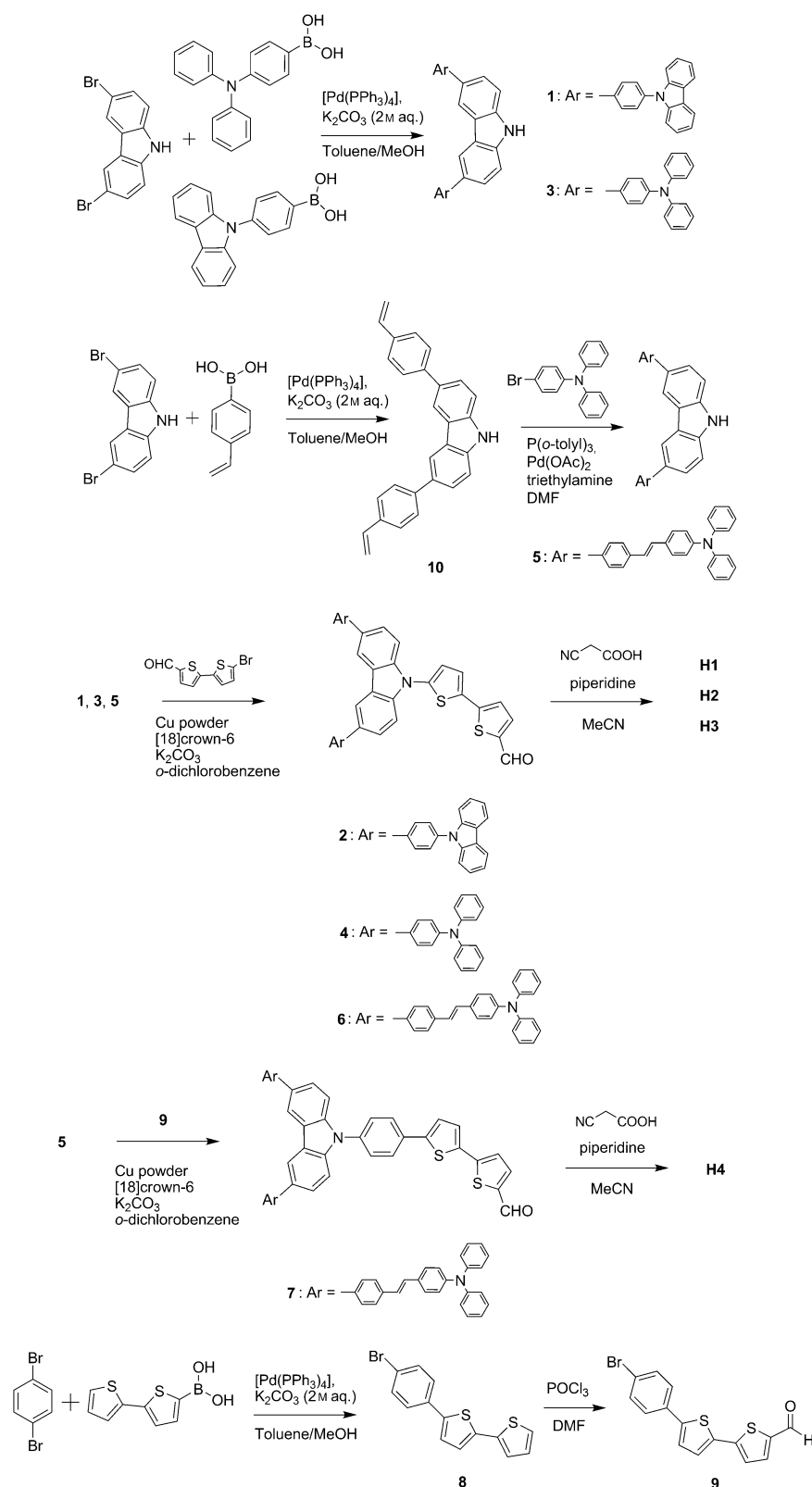
Scheme 2. Synthetic routes for **H1–H4**.

higher than the conduction band of TiO_2 (-0.5 V vs. NHE). Thus, these dyes show optimum energy levels for efficient electron transfer from an electrolyte to a nanocrystalline electrode.

To better understand the correlation between the molecular structure and the photophysical properties, we performed molecular orbital calculations using density functional theory. The ground state geometries of the H dyes were optimized in vacuum using the B3LYP/6-31G* level in the Gaussian 03 package. The optimized structures and isodensity plots of the frontier molecular orbitals are shown in Figure 2. The HOMO levels of the synthesized dyes are delocalized on the donor group consisting of TPA and the phenylcarbazole, extending to the carbazole core, and the LUMO is located mainly over the cyanoacrylic moiety and the dithiophene or phenyldithiophene. The well-separated orbital contributions in the electron density distribution of the HOMO and LUMO indicate efficient charge separation.

The photocurrent action spectra of **H1–H4** are shown in Figure 3. The DSCs were fabricated using a liquid electrolyte (0.6 M 1,2-dimethyl-3-n-propylimidazolium iodide, 0.05 M iodide, 0.1 M LiI, and 0.5 M 4-tert-butylpyridine in acetonitrile) and 12 μm-thick TiO_2 nanoparticles. We estimated the photovoltaic performance of the dyes with a black tape mask under standard global AM 1.5G solar radiation. The power conversion efficiencies for all the devices, except that using **H1**, exceeded 5%. Under the standard conditions, the device based on **H4** exhibited a short-circuit current density (J_{sc}) of

potential to 1.51 V versus NHE. The excited state oxidation potentials ($E_{0–0}*$) of the dyes are calculated from the equation $E_{0–0}* = E_{ox.} - E_{0–0}$. The calculated potentials are much

13.7 mA cm^{-2}, an open-circuit voltage (V_{oc}) of 0.68 V, a fill factor (FF) of 0.70, and a calculated efficiency of 6.52%. These results compare favorably with those obtained for a

FULL PAPERS

Table 1. Photophysical and electrochemical properties and photovoltaic performance[a] of the dyes **H1–H4** and N719.

Dye	λ_{abs} ($\varepsilon \times 10^4$ M^{-1} cm^{-1})[b] [nm]	λ_{max}[b] [nm]	E_{ox}[b] [V]	E_{0-0}[c] [V]	$E_{0-0}*$[d] [V]	J_{sc} [mA cm^{-2}]	V_{oc} [V]	FF [%]	η [%]
H1	309(5.28), 340(3.65), 393(2.90)	535	1.51	2.74	−1.23	6.32	0.53	0.72	2.41
H2	337(5.96), 393(2.83)	511	1.11	2.71	−1.60	12.2	0.60	0.77	5.64
H3	304(5.05), 386(9.69)	479	0.97	2.77	−1.80	13.0	0.63	0.75	6.14
H4	303(4.80), 390(10.1), 441(3.75)	519	1.01	2.65	−1.64	13.7	0.68	0.70	6.52
N719	–	–	–	–	–	14.7	0.68	0.73	7.30

[a] Measurements were based on a 0.11–0.13 cm^2 working area with a black mask on the fabricated cells. [b] Measured in DMF. Oxidation potentials were determined from the onset of cyclic voltammograms with a scan rate of 200 mV s^{-1}. Potentials were calibrated with the internal ferrocene standard ($E_{1/2}$ = +0.454 mV vs. Ag/AgNO$_3$). [c] The band gap E_{0-0} was derived from the onset of the absorption spectra. [d] $E_{0-0}*$ was calculated as E_{ox} − E_{0-0}.
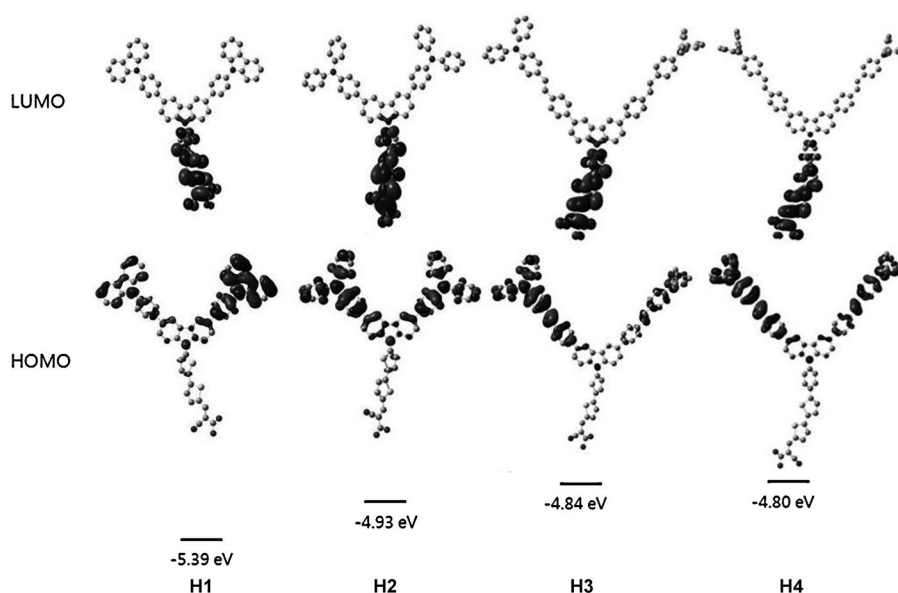
Figure 2. Computed isosurface plots of the frontier orbitals and energy states of sensitizers **H1–H4**.

reference cell based on JK-2 (7.22 %)[16g] and the commercially available N719 dye (7.30 %) under the same conditions. All the DSC devices fabricated using the H dyes have different J_{sc} and V_{oc} values. J_{sc} decreases in the following order: **H4** (13.7 mA cm^{-2}) > **H3** (13.0 mA cm^{-2}) > **H2** (12.2 mA cm^{-2}) > **H1** (6.32 mA cm^{-2}), which is explained by the trends observed in molar absorption coefficients and in the photoresponse regions of the dyes. As shown in Figure 3, the incident photon-to-electron conversion efficiency (IPCE) of **H4** shows a plateau around 400–550 nm and higher values than those of **H1–H3**. In addition, **H3** and **H4** exhibit a red-shifted IPCE spectrum up to 650 nm. This results from the extension of the π-conjugated system by incorporation of a vinylene-phenyl moiety at the 3- and 6-po-

sitions of the carbazole core and a phenyl unit at the bridge group in **H4**. The light absorption abilities of **H1** and **H2** are similar (see Figure 1), but **H1** has a more positive oxidation potential than **H2**; this inhibits efficient regeneration of the oxidized sensitizer. Moreover, TPA has a three-dimensional structure, in contrast to the planar carbazole moiety. This structure inhibits aggregation of the sensitizer on the TiO$_2$ particles, thereby resulting in a significantly high photocurrent. V_{oc} increases from **H1** to **H4**, which is related to charge transport from the dye to TiO$_2$ and the electron life time within the TiO$_2$ nanoparticles. To understand the correlation between V_{oc} and the donor unit, we measured electrochemical impedance spectra.[19] This method is generally used to investigate electron life times and photoinduced electron injection properties under open circuit and illuminated conditions. The second semicircle of the Nyquist plot (Figure S3 in the Supporting Information) indicates charge generation and transport. As shown in Figure S3, the order of the second semicircle radius decreases from **H1** (10.6 Ω) to **H4** (7.96 Ω), thus indicating that **H1** inhibits photoinduced electron injection to TiO$_2$ nanoparticles when compared with **H4**. In the Bode phase plot (Figure S3 in the Supporting Information), the middle-frequency peak (in the 10–100 Hz range) is indicative of the charge-transfer process of injected electrons in TiO$_2$. This finding is related to the electron life time and is ultimately correlated with V_{oc}. The electron life time is obtained from the middle-frequency peak (in the 10–100 Hz range) in the Bode phase plot using Equation (1), in which f is the frequency of the peak.

$$\tau = 1/2\pi f \tag{1}$$

The injected electron lifetime of the H dyes increases from **H1** (1.38 ms) to **H4** (5.66 ms). This result is correlated with the fact that **H2–H4**, which have a TPA moiety incorporated as a donor, possess higher V_{oc} values (0.60–0.68 V)
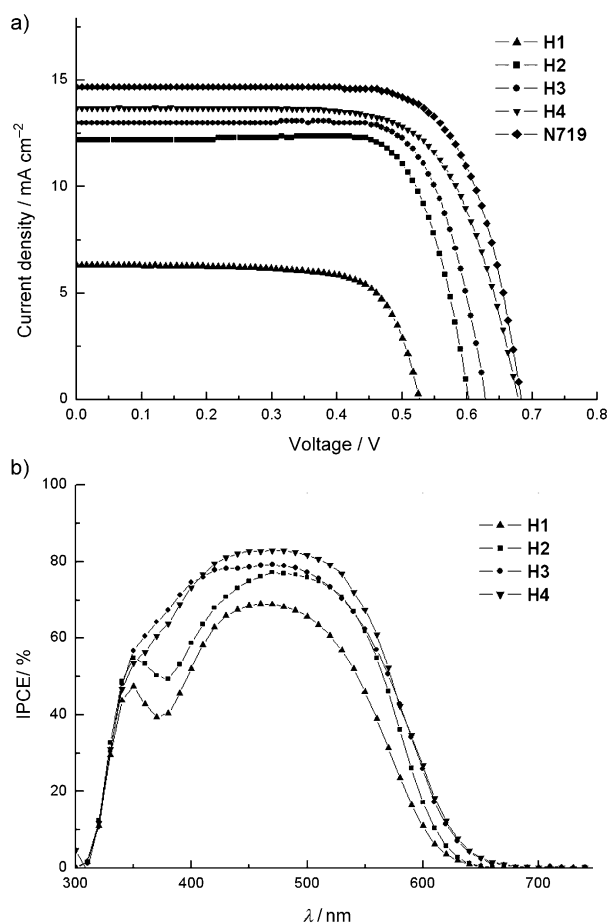
Figure 3. a) *I–V* curves and b) IPCE spectra of DSCs fabricated using **H1–H4**.

Figure 4. Variation of the photovoltaic parameters of **H4** under light soaking (AM 1.5G, 100 mWcm^{-2}) at 60°C.

than **H1** (0.53 V). The device based on **H4** showed the longest electron life time, which was four times longer than that of the **H1**-based device. Thus, the presence of a TPA unit in the H dyes as a donor increases not only charge generation and injection but also the electron life time, which improves V_{oc} and J_{sc}, and ultimately the photoconversion efficiency.

Because the long-term stability of devices is an important issue to evaluate commercial applications, we measured device performance using the **H4** dye with light soaking (AM 1.5G, 100 mWcm^{-2}) at 60°C, as shown in Figure 4. After 1000 hours of light soaking, the V_{oc} slightly decreases by 40 mV and the *FF* declines from 0.70 to 0.68, but the J_{sc} increases by 0.47 mAcm^{-2}. This enhancement of short-circuit current is likely the result of an improved percolation of the liquid electrolyte into cavities in the dye-adsorbed nanoporous TiO$_2$ layer that could not be accessed initially. Thus, the overall efficiency remains at 95% (6.15%) of the initial value (6.52%). These results suggest that the dye **H4** has potential for commercial applications.
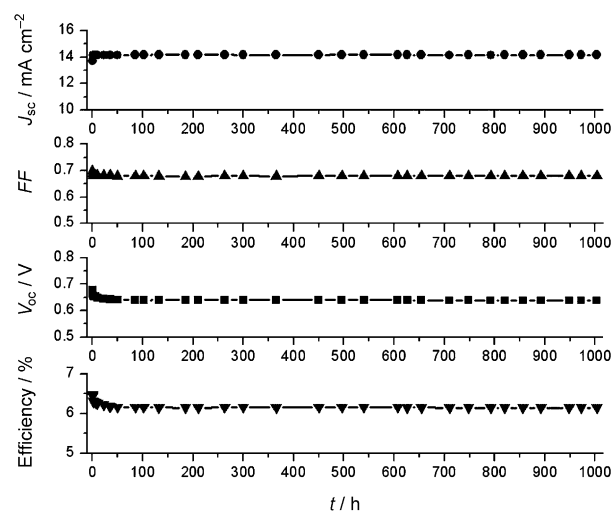
Conclusions

In summary, four organic dyes based on 3,6-disubstituted carbazole donors were synthesized and characterized regarding their efficiency in dye-sensitized solar cells. These dyes exhibited high molar extinction coefficients and energy levels suitable for electron transfer from an electrolyte to nanocrystalline TiO$_2$ particles. The device based on **H4** exhibited the highest conversion efficiency of 6.52%, which corresponds to approximately 89% of the conversion efficiency of cells based on the commercially available dye N719 (7.30%) under similar conditions. After 1000 hours of visible-light soaking at 60°C, the overall efficiency remained at 95% of the initial value. The results showed that **H4**, which featured the largest conjugation length, had the best light harvesting ability and long-term stability among the dyes investigated. Moreover, the triphenylamine unit as the donor was found more suitable for enhancing the efficiency than the carbazole moiety.

Experimental Section

General Information

All organic chemicals were purchased from Aldrich and TCI. Column chromatography was conducted on Merck silica gel 60 (70–230 mesh). All solvents and reagents were commercially available and used without further purification unless otherwise noted. ^{1}H and ^{13}C NMR spectra were recorded using an Avance 300- or 500 MHz Bruker spectrometer. UV/Vis spectra were recorded on a Beckman DU 650 spectrophotometer. Mass spectra were obtained using a gas chromatography–mass spectrometry instrument from JEOL (JMS-AX505WA, HP 5890 Series II) and a matrix-assisted laser desorption/ionization time-of-flight (MALDI-TOF) mass spectrometer from Bruker. Fluorescence spectra were recorded on a Jasco FP-7500 spectrophotometer. Cyclic voltammetry (CV) measurements were performed at room temperature on a CHI 660 Electrochemical Analyzer (CH Instruments, Inc., Texas, USA) using a solution of tetra-*n*-butylammonium hexafluorophosphate (Bu$_4$NPF$_6$, 0.1 M) in DMF as electrolyte solution. CV data were recorded using a reference electrode of Ag/Ag$^+$ (0.1 M AgNO$_3$ in acetonitrile) with a platinum wire

counter electrode at a scan rate of 200 mVs⁻¹. The absolute potential was calibrated to the NHE using an internal ferrocene/ferrocenium standard. The photovoltaic performances of the DSCs were measured using a 1000 W xenon light source, whose power as an AM 1.5 Oriel solar simulator was calibrated using a KG5-filtered Si reference solar cell. The incident photon-to-current conversion efficiency (IPCE) spectra for the cells were measured on an IPCE measuring system (PV Measurements). AC impedance measurements were performed under 1 sun illumination (100 mWcm⁻²) using an impedance analyzer (PARSTAT 2273, Princeton Applied Research USA).

Synthesis of 1, 3, 8, and 10

These compounds were prepared following the same protocol. Thus, only the synthesis of **1** is described. Spectral data for the other compounds are provided.

3,6-Bis(4-carbazol-9-yl-phenyl)-9H-carbazole (1)

A mixture of 3,6-dibromo-9H-carbazole (0.5 g, 1.57 mmol), 4-(9H-carbazol-9-yl)phenylboronic acid (1.00 g, 3.46 mmol), potassium carbonate (2 M aq., 50 mL), and tetrakis(triphenylphosphine)palladium (0.08 g, 0.06 mmol) in toluene was refluxed for 24 h. After cooling to room temperature, the reaction mixture was extracted with dichloromethane, and the organic phase was washed with H₂O and dried over Na₂SO₄. The solvent was evaporated to give the product, which was purified by silica-gel column chromatography and then recrystallized from dichloromethane and methanol to produce a green solid (yield: 417 mg, 41%). R_f = 0.357 (CH₂Cl₂/n-hexane = 1:1); ¹H NMR (300 MHz, CDCl₃): δ = 8.52 (s, 2H), 8.25 (s, 1H), 8.20 (d, 6 Hz, 4H), 7.99 (d, 6 Hz, 4H), 7.84 (d, 6 Hz, 2H), 7.71 (d, 6 Hz, 4H), 7.62 (d, 6 Hz, 2H), 7.54 (d, 6 Hz, 4H), 7.47 (t, 6 Hz, 4H), 7.33 ppm (t, 6 Hz, 4H); ¹³C NMR (125 MHz, CDCl₃): δ = 141.1, 140.9, 139.7, 136.2, 132.3, 128.6, 127.4, 126.0, 125.7, 124.1, 123.4, 120.4, 119.9, 119.0, 111.3, 109.9 ppm; MS (MALDI-TOF): m/z calcd for C₄₈H₃₁N₃: 649.252 [M+H]⁺; found: 649.443.

3,6-Bis-(4-diphenylamino-phenyl)-9H-carbazole (3)

This intermediate was prepared as described in a previous report.[20]

5-(4-Bromophenyl)-[2,2′]bithiophene (8)

R_f = 0.567 (CH₂Cl₂/n-hexane = 1:4); ¹H NMR (300 MHz, [D₆]acetone): δ = 7.65–7.62 (m, 4H), 7.50–7.46 (m, 2H), 7.34 (d, 1 Hz, 1H), 7.30 (d, 4 Hz, 1H), 7.12 ppm (t, 4 Hz, 1H); ¹³C NMR (125 MHz, CDCl₃): δ = 141.6, 137.2, 133.0, 132.0, 127.9, 127.0, 124.7, 124.6, 124.3, 124.1, 123.8, 121.3 ppm; MS (MALDI-TOF): m/z calcd for C₁₄H₉BrS₂: 319.933 [M+H]⁺; found: 320.149. This intermediate was reported in literature.[21]

3,6-Bis-(4-vinyl-phenyl)-9H-carbazole (10)

R_f = 0.464 (CH₂Cl₂/n-hexane = 1:1); ¹H NMR (300 MHz, [D₆]DMSO): δ = 11.4 (s, 1H), 8.63 (s, 2H), 7.82–7.71 (m, 6H), 7.60–7.56 (m, 6H), 6.85–6.75 (m, 2H), 5.89 (d, 12 Hz, 2H), 5.28 ppm (d, 12 Hz, 2H); ¹³C NMR (125 MHz, CDCl₃): δ = 141.4, 139.4, 136.5, 135.8, 132.6, 127.3, 126.7, 125.4, 124.0, 118.7, 113.5, 111.0 ppm; MS (MALDI-TOF): m/z calcd for C₂₈H₂₁N: 371.167 [M+H]⁺; found: 371.231.

Synthesis of 2, 4, 6, and 7

The preparation of these compounds followed similar protocols. Thus, only the synthesis of **2** is described. Spectral data for the other compounds are provided.

5′-[3,6-Bis-(4-carbazol-9-yl-phenyl)-carbazol-9-yl]-[2,2′]bithiophenyl-5-carbaldehyde (2)

ortho-Dichlorobenzene was added to a mixture of 3,6-bis(4-carbazol-9-yl-phenyl)-9H-carbazole (**1**) (0.3 g, 0.46 mmol), 5′-bromo-[2,2′]-bithiophenyl-5-carbaldehyde (0.14 g, 0.51 mmol), copper powder (0.02 g, 0.32 mmol), potassium carbonate (0.25 g, 1.84 mmol), and [18]crown-6 (0.04 g, 0.14 mmol). After the reaction mixture was refluxed for 48 h, it was cooled to room temperature. The reaction mixture was extracted with dichloromethane, and the organic phase was washed with H₂O and dried over Na₂SO₄. The solvent was removed to give the product, which

was purified by silica-gel column chromatography and then recrystallized from dichloromethane and methanol to produce a green oily product (yield: 280 mg, 72%). R_f = 0.310 (CH₂Cl₂/n-hexane = 2:1); ¹H NMR (300 MHz, CDCl₃): δ = 9.95 (s, 1H), 8.54 (s, 2H), 8.20 (d, 9 Hz, 4H), 7.99 (d, 9 Hz, 4H), 7.88 (d, 9 Hz, 2H), 7.77–7.71 (m, 6H), 7.56–7.44 (m, 10H), 7.38–7.31 ppm (m, 6H); ¹³C NMR (125 MHz, CDCl₃): δ = 182.5, 146.3, 142.2, 141.6, 140.9, 140.6, 139.6, 137.3, 136.5, 134.2, 133.9, 128.6, 127.4, 126.2, 126.0, 125.7, 125.0, 124.5, 123.4, 120.3, 120.0, 119.0, 110.9, 109.8 ppm; MS (MALDI-TOF): m/z calcd for C₅₇H₃₅N₃OS₂: 841.222 [M+H]⁺; found: 841.313.

5′-[3,6-Bis-(4-diphenylamino-phenyl)-carbazol-9-yl]-[2,2′]bithiophenyl-5-carbaldehyde (4)

R_f = 0.310 (CH₂Cl₂/n-hexane = 2:1); ¹H NMR (300 MHz, CDCl₃): δ = 9.92 (s, 1H), 8.34 (s, 2H), 7.72 (d, 9 Hz, 4H), 7.64–7.58 (d, 9 Hz, 6H), 7.47 (d, 3 Hz, 2H), 7.37–7.17 (m, 20H), 7.06 ppm (t, 7 Hz, 6H); ¹³C NMR (125 MHz, CDCl₃): δ = 182.5, 147.7, 146.8, 142.0, 141.0, 140.0, 137.3, 135.6, 134.3, 133.8, 129.3, 127.9, 125.7, 125.3, 125.0, 124.4, 124.3, 122.8, 118.4, 110.5 ppm; MS (MALDI-TOF): m/z calcd for C₅₇H₃₉N₃OS₂: 845.254 [M+H]⁺; found: 845.408.

5′-(3,6-Bis-[4-2-(4-diphenylamino-phenyl)-vinyl]-phenyl}-carbazol-9-yl)-[2,2′]bithiophenyl-5-carbaldehyde (6)

R_f = 0.310 (CH₂Cl₂/n-hexane = 2:1); ¹H NMR (300 MHz, CDCl₃): δ = 9.93 (s, 1H), 8.40 (s, 2H), 7.78–7.71 (m, 8H), 7.64 (d, 8 Hz, 5H), 7.56 (d, 8 Hz, 2H), 7.48 (d, 4 Hz, 2H), 7.45 (d, 8 Hz, 3H), 7.33–7.25 (m, 12H), 7.21–7.04 (m, 18H), 6.81 (q, 11 Hz, 6 Hz, 1H), 5.84 (d, 18 Hz, 1H), 5.31 ppm (d, 9 Hz, 1H); ¹³C NMR (125 MHz, CDCl₃): δ = 182.5, 147.5, 147.3, 146.4, 142.1, 141.3, 140.2, 139.8, 137.3, 136.3, 134.3, 133.9, 131.5, 129.3, 128.0, 127.4, 127.3, 126.8, 126.5, 125.9, 125.4, 125.0, 124.5, 123.6, 123.0, 118.6, 110.6 ppm; MS (MALDI-TOF): m/z calcd for C₇₃H₅₁N₃OS₂: 1049.347 [M+H]⁺; found: 1049.209.

5′-[4-(3,6-Bis-[4-2-(4-diphenylamino-phenyl)-vinyl]-phenyl}-carbazol-9-yl)-phenyl]-[2,2′]bithiophenyl-5-carbaldehyde (7)

R_f = 0.345 (CH₂Cl₂/n-hexane = 2:1); ¹H NMR (300 MHz, CDCl₃): δ = 9.88 (s, 1H), 8.40 (s, 2H), 7.87–7.62 (m, 12H), 7.55–7.36 (m, 7H), 7.32–7.20 (m, 9H), 7.19–7.02 (m, 19H), 6.81 (q, 11 Hz, 6 Hz, 1H), 5.85 (d, 18 Hz, 1H), 5.30 ppm (d, 9 Hz, 1H); ¹³C NMR (125 MHz, [D₆]DMSO): δ = 183.1, 145.0, 144.8, 143.3, 141.2, 141.1, 138.3, 134.6, 134.1, 132.6, 131.8, 131.7, 128.8, 127.9, 127.7, 127.6, 127.1, 125.5, 125.2, 124.9, 124.8, 124.7, 121.0 ppm; MS (MALDI-TOF): m/z calcd for C₇₉H₅₅N₃OS₂: 1125.379 [M+H]⁺; found: 1126.237.

5′-(4-Bromophenyl)-[2,2′]bithiophenyl-5-carbaldehyde (9)

POCl₃ (0.87 mL, 6.23 mmol) was added dropwise to DMF (2 mL) with stirring under dry conditions, and the temperature was kept below 10°C. Then compound **8** (1.00 g, 3.11 mmol) in dichloromethane (20 mL) was added to the reagent obtained from POCl₃ and DMF, the mixture was stirred overnight at room temperature. The reaction mixture was extracted with dichloromethane, and the organic phase was washed with H₂O and dried over Na₂SO₄. The solvent was removed to give the product, which was purified by silica-gel column chromatography to produce an orange solid (yield: 716 mg, 49%). R_f = 0.345 (CH₂Cl₂/n-hexane = 2:1); ¹H NMR (300 MHz, [D₆]acetone): δ = 9.95 (s, 1H), 7.96 (d, 3 Hz, 1H), 7.72–7.64 (m, 4H), 7.58–7.53 ppm (m, 3H); ¹³C NMR (125 MHz, [D₆]DMSO): δ = 184.3, 145.5, 143.9, 141.8, 139.6, 135.2, 132.5, 128.7, 127.8, 126.4, 125.8 ppm; MS (MALDI-TOF): m/z calcd for C₁₅H₉BrSO₂: 347.928 [M+H]⁺; found: 348.156.

3,6-Bis-[4-2-(4-diphenylamino-phenyl)-vinyl]-phenyl}-9H-carbazol (5)

A mixture of compound **10** (300 mg, 0.81 mmol), 4-bromotriphenylamine (654 mg, 2.02 mmol), palladium acetate (11.0 mg, 0.04 mmol), tri-o-tolylphosphine (50 mg, 0.16 mmol), and triethylamine in DMF (10 mL) was refluxed overnight. After cooling to room temperature, the solvent was evaporated under high vacuum, and the reaction mixture was extracted with dichloromethane. The organic phase was washed with water and dried over Na₂SO₄. The solvent was evaporated to give a crude mixture,

which was purified by silica-gel column chromatography and recrystallized from dichloromethane and hexane to produce a green solid (yield: 460 mg, 80%). $R_f = 0.393$ (CH_2Cl_2/n-hexane = 1:1); ^1H NMR (300 MHz, $CDCl_3$): $\delta = 8.34$ (s, 2H), 8.11 (s, 1H), 7.76–7.71 (m, 6H), 7.63 (d, 6 Hz, 4H), 7.54–7.44 (m, 8H), 7.32–7.27 (m, 6H), 7.17–7.04 (m, 17H), 6.88–6.77 (m, 1H), 5.85 (d, 18 Hz, 1H), 5.31 ppm (d, 9 Hz, 1H); ^{13}C NMR (125 MHz, $CDCl_3$): $\delta = 147.5$, 147.3, 140.8, 139.4, 135.9, 132.6, 131.6, 129.3, 127.8, 127.4, 127.3, 126.8, 126.7, 125.4, 124.5, 124.0, 123.6, 123.0, 118.6, 111.0 ppm; MS (MALDI-TOF): m/z calcd for $C_{64}H_{47}N_3$: 857.377 [M+H]$^+$; found: 857.349.

Synthesis of H1–H4

The preparation of these compounds followed similar protocols. Thus, only the synthesis of **H1** is described. Spectral data for the other compounds are provided.

3-[5′-[3,6-Bis-(4-carbazol-9-yl-phenyl)-carbazol-9-yl]-[2,2′]bithiophenyl-5-yl]-2-cyano-acrylic acid (H1)

A mixture of compound **2** (150 mg, 0.18 mmol) and cyanoacetic acid (23 mg, 0.27 mmol) was dissolved in 50 mL of MeCN and 50 mL of THF containing piperidine (46 mg, 0.54 mmol). The reaction mixture was refluxed overnight. After cooling, 1 N HCl was added to the reaction mixture for neutralization, and the reaction mixture was extracted with dichloromethane. The organic phase was washed with water and dried over Na_2SO_4. The solvent was evaporated to give the crude mixture, which was purified by silica-gel column chromatography to give a reddish-brown solid product (yield: 120 mg, 73%). $R_f = 0.309$ ($CH_2Cl_2/MeOH/AcOH = 10:1:0.1$); ^1H NMR (300 MHz, [D_6]DMSO): $\delta = 8.94$ (s, 2H), 8.28 (d, 8 Hz, 4H), 8.15 (d, 8 Hz, 4H), 8.09 (s, 1H), 8.00 (d, 9 Hz, 2H), 7.80–7.76 (m, 6H), 7.72 (d, 4 Hz, 1H), 7.68 (d, 4 Hz, 1H), 7.58 (d, 3 Hz, 2H), 7.51–7.44 (m, 8H), 7.32 ppm (t, 6 Hz, 4H). ^{13}C NMR (500 MHz, [D_6]DMSO): $\delta = 143.4$, 142.0, 141.8, 141.0, 140.5, 138.4, 137.6, 136.6, 136.3, 134.7, 134.5, 134.4, 134.2, 133.6, 129.2, 127.9, 127.1, 126.7, 125.8, 125.6, 125.0, 123.7, 121.4, 120.9, 120.2, 118.9, 111.7, 110.6 ppm; MS (HRMS): m/z calcd for $C_{60}H_{36}N_4O_2S_2$: 909.2355 [M+H]$^+$; found: 909.2358.

3-[5′-[3,6-Bis-(4-diphenylamino-phenyl)-carbazol-9-yl]-[2,2′]bithiophenyl-5-yl]-2-cyano-acrylic acid (H2)

$R_f = 0.309$ ($CH_2Cl_2/MeOH/AcOH = 10:1:0.1$); ^1H NMR (300 MHz, [D_6]DMSO): $\delta = 8.63$ (s, 2H), 8.12 (s, 1H), 7.75–7.69 (m, 7H), 7.60 (d, 7 Hz, 3H), 7.53 (d, 4 Hz, 1H), 7.45 (d, 4 Hz, 1H), 7.31 (t, 8 Hz, 9H), 7.09–7.04 ppm (m, 16H). ^{13}C NMR (500 MHz, [D_6]DMSO): $\delta = 147.6$, 146.6, 141.1, 140.7, 138.1, 136.6, 136.5, 135.2, 133.8, 133.6, 130.5, 129.9, 128.2, 128.1, 126.3, 125.8, 125.4, 125.2, 124.9, 124.4, 124.3, 123.4, 119.6, 119.0, 111.9, 110.9 ppm; MS (HRMS): m/z calcd for $C_{60}H_{40}N_4O_2S_2$: 913.2670 [M+H]$^+$; found: 913.2671.

3-[5′-(3,6-Bis-[4-[2-(4-diphenylamino-phenyl)-vinyl]-phenyl]-carbazol-9-yl)-[2,2′]bithiophenyl-5-yl]-2-cyano-acrylic acid (H3)

$R_f = 0.364$ ($CH_2Cl_2/MeOH/AcOH = 10:1:0.1$); ^1H NMR (300 MHz, [D_6]DMSO): $\delta = 8.69$ (s, 2H), 8.10 (s, 1H), 7.78 (d, 8 Hz, 6H), 7.66 (d, 8 Hz, 5H), 7.59 (d, 8 Hz, 4H), 7.52 (d, 8 Hz, 4H), 7.44 (d, 9 Hz, 2H), 7.31 (t, 7 Hz, 8H), 7.20 (d, 9 Hz, 3H), 7.08–7.01 (m, 12H), 6.95 ppm (d, 8 Hz, 4H). ^{13}C NMR (500 MHz, [D_6]DMSO): $\delta = 147.3$, 147.1, 141.0, 140.9, 140.3, 140.2, 139.6, 139.5, 137.9, 136.7, 136.3, 133.9, 133.5, 131.9, 130.0, 128.1, 128.0, 127.3, 127.1, 126.8, 126.4, 125.9, 125.4, 125.2, 124.6, 124.4, 123.6, 123.4, 119.6, 119.2, 112.7, 111.0 ppm. MS (HRMS): m/z calcd for $C_{76}H_{52}N_4O_2S_2$: 1117.3627 [M+H]$^+$; found: 1117.3610.

3-[5′-[4-(3,6-Bis-[4-[2-(4-diphenylaminophenyl)vinyl]-phenyl]-carbazol-9-yl)-phenyl]-[2,2′]bithiophenyl-5-yl]-2-cyanoacrylic acid (H4)

$R_f = 0.364$ ($CH_2Cl_2/MeOH/AcOH = 10:1:0.1$); ^1H NMR (300 MHz, [D_6]DMSO): $\delta = 8.76$ (s, 2H), 8.05 (s, 1H), 7.98 (d, 7 Hz, 2H), 7.76–7.61 (m, 6H), 7.68–7.60 (m, 9H), 7.54–7.46 (m, 8H) 7.31 (t, 7 Hz, 8H), 7.21 (d, 9 Hz, 3H), 7.09–7.02 (m, 12H), 6.95 ppm (d, 8 Hz, 4H). ^{13}C NMR (500 MHz, [D_6]DMSO): $\delta = 147.4$, 147.1, 143.1, 140.3, 139.8, 136.8, 136.2, 136.1, 135.9, 132.6, 132.5, 130.2, 130.0, 128.0, 127.7, 127.4, 127.3, 127.2, 127.1, 127.0, 126.9, 126.2, 125.9, 125.5, 125.0, 124.9, 124.5, 124.3, 123.9, 123.6, 123.4, 119.9, 119.1, 111.4, 110.7 ppm. MS (HRMS): m/z calcd for $C_{82}H_{56}N_4O_2S_2$: 1193.3947 [M+H]$^+$; found: 1193.3923.

Device fabrication of dye-sensitized solar cells

Fluorine-doped tin oxide (FTO) glass plates (Pilkington, 8 Ω sq^{-1}, 2.3 mm thick) were cleaned in a detergent solution using an ultrasonic bath for 15 min and then rinsed with water and ethanol. The washed FTO glass plates were immersed in an aqueous 40 mM $TiCl_4$ solution for 30 min at 70°C. A transparent nanocrystalline layer was deposited on the FTO glass by the doctor blade printing method using TiO_2 paste (Ti-Nanoxide T/SP, Solaronix) and a scattering layer paste (CCIC, PST-400C). The TiO_2 layer was gradually sintered according to a programmed procedure. The sintered layer consisted of a 10 mm-thick transparent layer and 4 mm-thick scattering layer. The TiO_2 electrodes were treated again with $TiCl_4$ at 70°C for 30 min and sintered at 500°C for 30 min. After the TiO_2 electrodes were immersed in 0.3 mM dye solution in DMF containing 10 mM 3α,7α-dihydroxy-5β-cholic acid, they were kept at room temperature for 18 h in the dark. The FTO plate for the counter electrode was cleaned in an ultrasonic bath containing H_2O, acetone, and 0.1 M HCl aqueous solution. Subsequently, counter electrodes were prepared by coating with a drop of H_2PtCl_6 solution (2 mg of Pt in 1 mL of ethanol) on an FTO plate followed by heating at 400°C for 15 min. The dye-adsorbed TiO_2 electrode was then attached to the counter electrode by heating with a hot-melt polymer film (Surlyn 1702, 100 mm thick, DuPont). A drop of electrolyte solution (0.6 M 1,2-dimethyl-3-n-propyl-imidazolium iodide, 0.05 M iodine, 0.1 M LiI, and 0.5 M 4-$tert$-butylpyridine in acetonitrile) was permeated through a hole in the counter electrode, which was driven into the cell by vacuum backfilling. Finally, the hole was sealed using a hot-melt polymer film with a cover glass (0.1 mm thick). N719 was purchased from Solaronix.

Acknowledgements

[1] N. Robertson, *Angew. Chem.* **2006**, *118*, 2398; *Angew. Chem. Int. Ed.* **2006**, *45*, 2338.

[2] a) M. Grätzel, *Nature* **2001**, *414*, 338; b) B. O'Regan, M. Grätzel, *Nature* **1991**, *353*, 737; c) Z. Ning, Y. Fu, H. Tian, *Energy Environ. Sci.* **2010**, *3*, 1170.

[3] a) A. B. F. Martinson, T. Hamann, M. Pellin, J. Hupp, *Chem. Eur. J.* **2008**, *14*, 4458; b) T. Daeneke, T.-H. Kwon, A. B. Holmes, N. W. Duffy, U. Bach, L. Spiccia, *Nat. Chem.* **2011**, *3*, 213.

[4] M. K. Nazeeruddin, A. Kay, I. Rodicio, R. Humphry-Baker, E. Müller, P. Liska, N. Vlachopoulos, M. Grätzel, *J. Am. Chem. Soc.* **1993**, *115*, 6382.

[5] A. Mishra, M. K. R. Fischer, P. Bäuerle, *Angew. Chem.* **2009**, *121*, 2510; *Angew. Chem. Int. Ed.* **2009**, *48*, 2474.

[6] a) M. K. Nazeeruddin, F. De Angelis, S. Fantacci, A. Selloni, G. Viscardi, P. Liska, S. Ito, B. Takeru, M. Grätzel, *J. Am. Chem. Soc.* **2005**, *127*, 16835; b) M. Grätzel, *J. Photochem. Photobiol. A* **2004**, *164*, 3.

[7] M. K. Nazeeruddin, P. Péchy, T. Renouard, S. M. Zakeeruddin, R. Humphry-Baker, P. Comte, P. Liska, L. Cevey, E. Costa, V. Shklover, L. Spiccia, G. B. Deacon, C. A. Bignozzi, M. Grätzel, *J. Am. Chem. Soc.* **2001**, *123*, 1613.

[8] S. Ko, H. Choi, M.-S. Kang, H. Hwang, H. Ji, J. Kim, J. Ko, Y. Kang, *J. Mater. Chem.* **2010**, *20*, 2391.

[9] T. Horiuchi, H. Miura, K. Sumioka, S. Uchida, *J. Am. Chem. Soc.* **2004**, *126*, 12218.

[10] a) M. Miyashita, K. Sunahara, T. Nishikawa, Y. Uemura, N. Koumura, K. Hara, A. Mori, T. Abe, E. Suzuki, S. Mori, *J. Am. Chem. Soc.* **2008**, *130*, 17874; b) J. Tang, J. Hua, W. Wu, H. Tian, *Energy Environ. Sci.* **2010**, *3*, 1736; c) B. Liu, W. Zhu, H. Tian, *Chem. Commun.* **2009**, 1766.

[11] a) K. Hara, K. Sayama, Y. Ohga, A. Shinpo, S. Suga, H. Arakawa, *Chem. Commun.* **2001**, 569; b) A. Furube, R. Katoh, K. Hara, T. Sato, S. Murata, H. Arakawa, M. Tachiya, *J. Phys. Chem. B* **2005**, *109*, 16406; c) K. Hara, T. Sato, R. Katoh, A. Furube, Y. Ohga, A. Shinpo, S. Suga, K. Sayama, H. Sugihara, H. Arakawa, *J. Phys. Chem. B* **2003**, *107*, 597; d) K. Hara, Z. S. Wang, T. Sato, A. Furube, R. Katoh, H. Sugihara, Y. Dan-Oh, C. Kasada, A. Shinpo, S. Suga, *J. Phys. Chem. B* **2005**, *109*, 15476; e) Z. S. Wang, Y. Cui, Y. Dan-oh, C. Kasada, A. Shinpo, K. Hara, *J. Phys. Chem. C* **2007**, *111*, 7224.

[12] a) S. Ito, H. Miura, S. Uchida, M. Takata, K. Sumioka, P. Liska, P. Comte, P. Pechy, M. Grätzel, *Chem. Commun.* **2008**, 5194; b) S. Ito, S. M. Zakeeruddin, R. Humphry-Baker, P. Liska, R. Charvet, P. Comte, M. K. Nazeeruddin, P. Pechy, M. Takata, H. Miura, S. Uchida, M. Grätzel, *Adv. Mater.* **2006**, *18*, 1202.

[13] a) A. J. Mozer, P. Wagner, D. L. Officer, G. G. Wallace, W. M. Campbell, M. Miyashita, K. Sunahara, S. Mori, *Chem. Commun.* **2008**, 4741; b) M. K. Nazeeruddin, R. Humphry-Baker, D. L. Officer, W. M. Campbell, A. K. Burrell, M. Grätzel, *Langmuir* **2004**, *20*, 6514.

[14] a) K. Sayama, S. Tsukagoshi, K. Hara, Y. Ohga, A. Shinpou, Y. Abe, S. Suga, H. Arakawa, *J. Phys. Chem. B* **2002**, *106*, 1363; b) K. Sayama, S. Tsukagoshi, T. Mori, K. Hara, Y. Ohga, A. Shinpou, Y. Abe, S. Suga, H. Arakawa, *Sol. Energy Mater. Sol. Cells* **2003**, *80*, 47.

[15] a) J.-H. Yum, P. Walter, S. Huber, D. Rentsch, T. Geiger, F. Nüesch, F. De Angelis, M. Grätzel, M. K. Nazeeruddin, *J. Am. Chem. Soc.* **2007**, *129*, 10320; b) S. Tatay, S. A. Haque, B. O'Regan, J. R. Durrant, W. J. H. Verhees, J. M. Kroon, A. Vidal-Ferran, P. Gavina, E. Palomares, *J. Mater. Chem.* **2007**, *17*, 3037; c) A. Burke, S. Ito, H. Snaith, U. Bach, J. Kwiatkowski, M. Gratzel, *Nano Lett.* **2008**, *8*, 977; d) Y. Chen, Z. Zeng, C. Li, W. Wang, X. Wang, B. Zhang, *New J. Chem.* **2005**, *29*, 773; e) T. Geiger, S. Kuster, J.-H. Yum, S.-J. Moon, M. K. Nazeeruddin, M. Grätzel, F. Nüesch, *Adv. Funct. Mater.* **2009**, *19*, 2720.

[16] a) H. Choi, C. Baik, S. O. Kang, J. J. Ko, M. S. Kang, M. K. Nazeeruddin, M. Grätzel, *Angew. Chem.* **2008**, *120*, 333; *Angew. Chem. Int. Ed.* **2008**, *47*, 327; b) K. Hara, M. Kurashige, S. Ito, A. Shinpo, S. Suga, K. Sayama, H. Arakawa, *Chem. Commun.* **2003**, 252; c) S. L. Li, K. J. Jiang, K. F. Shao, L. M. Yang, *Chem. Commun.* **2006**, 2792; d) R. Chen, X. Yang, H. Tian, X. Wang, A. Hagfeldt, L. Sun, *Chem. Mater.* **2007**, *19*, 4007; e) K. R. J. Thomas, Y.-C. Hsu, J. T. Lin, K.-M. Lee, K.-C. Ho, C. H. Lai, Y.-M. Cheng, P.-T. Chou, *Chem. Mater.* **2008**, *20*, 1830; f) Z. S. Wang, N. Koumura, Y. Cui, M. Takahashi, H. Sekiguchi, A. Mori, T. Kubo, A. Furube, K. Hara, *Chem. Mater.* **2008**, *20*, 3993; g) S. Kim, J. W. Lee, S. O. Kang, J. Ko, J. H. Yum, S. Fantacci, F. De Angelis, D. Di Censo, M. K. Nazeeruddin, M. Grätzel, *J. Am. Chem. Soc.* **2006**, *128*, 16701; h) N. Koumura, Z. S. Wang, S. Mori, M. Miyashita, E. Suzuki, K. Hara, *J. Am. Chem. Soc.* **2006**, *128*, 14256; i) H. Qin, S. Wenger, M. Xu, F. Gao, X. Jing, P. Wang, S. M. Zakeeruddin, M. Grätzel, *J. Am. Chem. Soc.* **2008**, *130*, 9202; j) N. Cho, H. Choi, D. Kim, K. Song, M.-S. Kang, S. O. Kang, J. Ko, *Tetrahedron* **2009**, *65*, 6236; k) Z. Ning, Q. Zhang, W. Wu, H. Pei, B. Liu, H. Tian, *J. Org. Chem.* **2008**, *73*, 3791; l) W. Zhu, Y. Wu, S. Wang, W. Li, X. Li, J. Chen, Z.-S. Wang, H. Tian, *Adv. Funct. Mater.* **2011**, *21*, 756; m) W. Wu, J. Yang, H. Tian, *J. Mater. Chem.* **2010**, *20*, 1772; n) T.-H. Kwon, V. Armel, A. Nattestad, D. R. MacFarlane, U. Bach, S. J. Lind, K. C. Gordon, W.a Tang, D. J. Jones, A. B. Holmes, *J. Org. Chem.* **2011**, *76*, 4088.

[17] W. Zeng, Y. Cao, Y. Bai, Y. Wang, Y. Shi, M. Zhang, F. Wang, C. Pan, P. Wang, *Chem. Mater.* **2010**, *22*, 1915.

[18] a) S. Roquet, A. Cravino, P. Leriche, O. Alévêque, P. Frère, J. Roncali, *J. Am. Chem. Soc.* **2006**, *128*, 3459; b) Y. Shirota, *J. Mater. Chem.* **2000**, *10*, 1 – 25; c) J. He, W. Wu, J. Hua, Y. Jiang, S. Qu, J. Li, Y. Long, H. Tian, *J. Mater. Chem.* **2011**, *21*, 6054; d) Z. Ning, H. Tian, *Chem. Commun.* **2009**, 5483.

[19] a) R. Kern, R. Sastrawan, J. Ferber, R. Stangl, J. Luthet, *Electrochim. Acta* **2002**, *47*, 4213; b) L.-Y. Lin, C.-H. Tsai, K.-T. Wong, T.-W. Huang, L. Hsieh, S.-H. Liu, H.-W. Lin, C.-C. Wu, S.-H. Chou, S.-H. Chen, A.-I Tsai, *J. Org. Chem.* **2010**, *75*, 4778; c) M. Velusamy, Y.-C. Hsu, J. T. Lin, C.-W. Chang, C.-P. Hsu, *Chem. Asian J.* **2010**, *5*, 87; d) H. Choi, J.-J. Kim, K. Song, J. Ko, M. K. Nazeeruddin, M. Grätzel, *J. Mater. Chem.* **2010**, *20*, 3280.

[20] a) P. F. Xia, J. Lu, C. H. Kwok, H. Fukutani, M. S. Wong, Y. Tao, *J. Polym. Sci., Part A: Polym. Chem.* **2009**, *47*, 137; b) Z. H. Li, M. S. Wong, *Org. Lett.* **2006**, *8*, 1499.

[21] W. Liu, M. Pink, D. Lee, *J. Am. Chem. Soc.* **2009**, *131*, 8703.